Polystyrene- and Poly(3-vinylpyridine)-Grafted Magnetite Nanoparticles Prepared through Surface-Initiated Nitroxide-Mediated Radical Polymerization

Ryosuke Matsuno, Kazuya Yamamoto, Hideyuki Otsuka, and Atsushi Takahara*

Institute for Materials Chemistry and Engineering, Kyushu University, Hakozaki, Higashi-ku, Fukuoka 812-8581, Japan

Received October 9, 2003; Revised Manuscript Received January 14, 2004

ABSTRACT: Polymer-grafted magnetite (Fe_3O_4) nanoparticles (diameter about 10 nm) were prepared through a direct polymer grafting reaction from their surfaces. The chemisorbed initiator (TEMPO-based alkoxyamine) for nitroxide-mediated radical polymerization with a phosphoric acid group gave controlled polystyrene (PS) and poly(3-vinylpyridine) (P3VP) graft layers on the surface. The graft densities of polymers on the surfaces of magnetite particles were estimated at 0.12−0.20 chains/nm^2 by thermogravimetric analysis (TGA). The improvement in the dispersibility of PS-modified magnetite in good solvents was verified by ultraviolet−visible (UV−vis) absorption spectroscopy, transmission electron microscopy (TEM), and dynamic light scattering (DLS). In the case of P3VP-modified magnetite, the particles were stably dispersed in good solvents, by protonation, in acid solution, and by quarternization with iodomethane, in neutral aqueous solution. The magnetic response of the polymer-grafted magnetite against an external magnetic field was confirmed in the stable dispersion.

Introduction

Surface modification of nanoparticles allows for the dispersion and stability of these nanoparticles in various solvents or polymer matrices while they maintain their physical characteristics. In the field of clay nanocomposites, the surface modification of clay nanofiller using a small organic molecule has been reported.[1] This method achieves stable dispersion of layered silicate clay nanofiller in a polymer matrix by exfoliation accompanying adsorption of the organic molecule with high affinity to a matrix on the nanofiller surface and an improvement in the characteristics of polymer nanocomposites for nanodispersion.

The modification technique frequently employed makes use of the interaction between the nanoparticle surface and the functional groups of organic molecules, for example silica particles and a silane coupling agent,[2] gold particles and a functionalized thiol group,[3] and so on. Because the surface of metal oxide particles consists of metal−OH groups, a widely applicable surface modification technique is required. The authors have previously reported on surface modification using the specific interaction between the Al−OH groups of inorganic nanofiber surfaces and *n*-octadecylphosphonic acid.[4] Utilizing the interaction between the metal−OH and the phosphonic acid groups is a promising approach to the surface modification of metal oxide nanoparticles in general.[5]

Surface modification using polymers has recently been reported. Surface grafting of polymers is one of the most effective methods of achieving these surface modifications, as the surface properties can be widely changed by a variety of functional monomers. There are two types of methods for surface modification using polymers. One is a "grafted-to" system[6] in which polymers are adsorbed onto the substrate surface and nanoparticle surface after polymerization. The other is a "grafted-from" system in which the surface-initiated polymerization is carried out on the substrate surface and nanoparticle surface. The "grafted-from" method usually results in poor control of molecular weight and molecular weight distribution.[7,8] Recently, surface-initiated graft polymerization to control these molecular weight factors using living radical polymerization techniques has been reported.[9−11]

In the present study, "grafted-from" surface modification using nitroxide-mediated radical polymerization (NMRP)[12] was performed so as to achieve high graft density. Magnetite (Fe_3O_4) with magnetic properties was employed as a nanoparticle. Magnetic particles have been widely used in the study of in vivo biomedical applications, including magnetic resonance imaging,[13] ferrofluids,[14−16] nanoscale magnetooptic phenomena,[17] and markers of antigen-antibodies[18] due to their attractive magnetic properties.

The authors report herein the preparation of polymer-grafted magnetic particles using the interaction between Fe−OH on the magnetite nanoparticle surface and phosphoric acid groups. Furthermore, the dispersibility of polymer-grafted magnetite and the magnetic response against an external magnetic field in various solvents was investigated.

Experimental Section

Materials. Magnetite particles with diameters of 10 nm were provided by Prof. K. Enpuku (Kyushu University). Styrene was obtained from WAKO Pure Chemical Industries, Ltd., and purified by distillation under reduced pressure over calcium hydride. 3-Vinylpyridine was synthesized by a previously reported method[19] and purified by distillation under reduced pressure over calcium hydride.

Measurements. Gel permeation chromatographic (GPC) analysis was carried out at 313 K on a Tosoh HLC-8120GPC with a guard column (Shodex GPC KF-804L), and a differential refractometer RI-8020. Tetrahydrofuran (THF) was used as

* To whom correspondence should be addressed.Telephone: +81-92-642-2721. Fax: +81-92-642-2715. E-mail: takahara@cstf.kyushu-u.ac.jp.

10.1021/ma035523g CCC: $27.50
Published on Web 02/17/2004

Scheme 1. Molecular Design and Synthesis of Surface Modifier with Nitroxide-Mediated Radical Polymerization Initiator Moiety

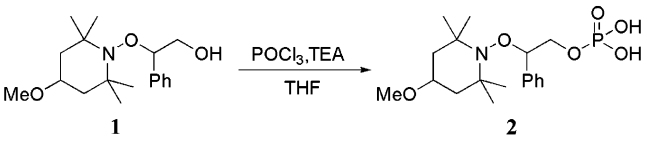

an eluent for PS analysis. THF containing 5 vol % *N*,*N*,*N*′,*N*′-tetramethylethylenediamine was used as an eluent for P3VP analysis. PS standards were used to calibrate the GPC system. ^{1}H NMR spectra were recorded on a JNM-EX-400 (JEOL). FTIR spectroscopy (KBr pellet) was recorded by Spectrum One (Perkin-Elmer Japan Co., Ltd.) at a resolution of 1 cm^{-1}. Thermogravimetric analysis (TGA) was performed by Thermo Plus 2 (Rigaku Corporation), using aluminum plates with ca. 2 mg of the sample under a nitrogen atmosphere and a heating rate of 10 K/min. Ultraviolet−visible (UV−vis) absorption spectra were recorded by Lambda 35 (Perkin-Elmer Japan Co., Ltd.). Transmission electron microscopy (TEM) observations were made on an H-7500 (HITACHI) operated at 100 kV. Dynamic light scattering (DLS) measurements were performed by DLS-7000 (Otsuka Electronics Co., Ltd.) at 13−20 mW of Ar laser.

Synthesis of Surface Initiator (Scheme 1). To realize direct polymerization of styrene from the surface of magnetite, a surface modifier with a nitroxide-mediated initiator group known for living free radical polymerization was employed. As shown in Scheme 1, the designed modifier **2** has both a NMRP moiety that contains 2,2,6,6-tetramethylpiperidinyl-1-oxyl (TEMPO), as reported by Hawker,[12] and a phosphoric acid moiety that can be expected to interact with metal−OH groups. Surface modifier **2** was synthesized from precursor **1**. The synthesis of compound **1** was conducted following the methods described in refs 12 and 20.The synthesis of compound **2** was carried out by the following method. A mixture of **1**, triethylamine (TEA), and THF was added to THF solution of $POCl_3$ at 273 K. The mixture was stirred for 2 h at room temperature. The solvent was then evaporated, and chloroform was used for extraction. Surface modifier **2** was separated by silica gel chromatography (chloroform−ethyl acetate−methanol) and obtained in 33% yields. The structure of **2** was confirmed by ^{1}H NMR and IR spectra.

2. ^{1}H NMR (400 MHz, DMSO): 0.64 (s, 3H), 1.14 (s, 3H), 1.29 (s, 3H), 1.46 (s, 3H), 1.14−1.98 (m, 4H), 3.28 (s, 3H), 3.75 (s, 1H), 4.03 (s, 1H), 4.37 (s, 1H), 4.88 (t, J = 6 Hz 1H), 7.40−7.43 (m, aromatic) ppm. FT-IR (KBr, cm^{-1}): 3424, 2979, 2945, 2815, 2605,1172, 763, 700.

Preparation of Initiator-Coated Magnetite. Adsorption of **2** onto the magnetite surface was conducted as follows. Magnetite (d = 10 nm) and **2** (1:1, w/w) were added to THF, and the suspension was sonicated for 24 h with cooling and then centrifuged, decanted, and rinsed with ethanol several times to remove the nonchemisorbed **2**. The amount of adsorbed **2** on the nanoparticle surfaces, as estimated by TGA, was 0.055 mg per 1 mg of magnetite particles. The calculated amount of **2** at the complete monolayer coverage of the magnetite surface was estimated to be 0.067 mg. The degree of coverage of **2** on the magnetite surface was 82%.

Results and Discussion

Surface-Initiated NMRP of Styrene on Magnetite. Polymerization of styrene on the surface of magnetite nanoparticles was carried out by heating a mixture of modified magnetite particles (3.0 mg), free initiator (4-hydroxy-1-((2′-hydroxy-1′-phenylethyl)oxy)-2,2,6,6-tetramethylpiperidine),[21] and styrene at 398 K (Scheme 2), after degassing by four freeze−pump−thaw cycles. Free initiator was used for control of molecular weights and estimation of molecular weight of grafted P3VP on magnetite nanoparticles. In the case of PS, polymerization was performed at 523:1 ratio of monomer to free initiator. After polymerization, unreacted styrene monomer was removed by washing with chloroform, and the dispersed magnetite was collected by applying a magnetic field. The PS polymerized by free initiator was recovered by reprecipitation in methanol. The grafted PS on the magnetite surface was collected by dissolving the magnetite core by hydrochloric acid (37%). The number-average molecular weights (M_n) and polydispersities (M_w/M_n) of the grafted PS and the PS recovered from the free initiator were evaluated by GPC measurements.

Table 1 shows M_n and M_w/M_n of the grafted PS and the PS polymerized by free initiator. M_n of the grafted PS, which was evaluated after dissolving the magnetite core with hydrochloric acid (37%), and of the PS derived from the free initiator were almost the same at relatively low monomer conversion (nos. 1 and 2). M_w/M_n values were also almost the same between the grafted PS and the PS polymerized by free initiator. At high monomer conversion and low M_w/M_n values, M_n of the grafted PS and the PS polymerized by free initiator were slightly different (no. 3). Therefore, in the case of relatively low M_w/M_n values of free polymer, M_w/M_n values of the grafted polymer are conjectured to be equivalent. These results indicate that the nitroxide-mediated initiator adsorbed on the magnetite surface by the interaction between Fe−OH and phosphoric acid groups successfully initiated the radical polymerization of styrene.

Surface-Initiated NMRP of 3-Vinylpyridine on Magnetite. Polymerization of 3VP monomer as well as that of styrene was carried out on the surface of magnetite nanoparticles. In the case of 2-vinylpyridine (2VP), it has been reported that when 2VP is polymerized by TEMPO-end-capped PS-type initiator at 398 K, the polymerization of 2VP is not controllable.[22] Furthermore, 3VP can be polymerized in a controlled manner with nitroxide, and the influence of temperature and nitroxide concentrations is quite logical.[19] For these reasons, 3VP was used as the vinylpyridine in this study. After polymerization, unreacted 3VP monomer was removed by washing with chloroform, and the magnetite-dispersed solution was collected by applying a magnetic field. The P3VP polymerized from free initiator was recovered by reprecipitation in hexane. The grafted P3VP was also isolated by dissolving the magnetite core with concentrated HCl (37%). However, we found that it is difficult to neutralize completely protonated P3VP to dissolve in THF to estimate the molecular weight by GPC. Therefore, the M_n and M_w/M_n of the grafted P3VP were evaluated by GPC measurement of the free polymer produced from the free initiator.

Table 2 shows M_n and M_w/M_n of the P3VP recovered from the free initiator. In the P3VP, M_n was not controlled at a 523:1 ratio of monomer to free initiator, and M_w/M_n were broad because the polymerization rates were so fast that the viscosity increased (nos. 1 and 2). When the ratio of monomer to free initiator was 350:1 (nos. 3 and 4), M_n was relatively controlled and M_w/M_n became relatively narrower compared with no. 1 and no. 2.

Determination of Graft Density of Polymer on Magnetite. Table 3 shows the graft densities σ (chains/nm^2) of representative PS or P3VP on magnetite particles. The graft density was calculated from the weight loss of polymer on nanoparticles by TGA, and the

Scheme 2. Surface Modification of Magnetite with 2 and Surface-Initiated NMRP

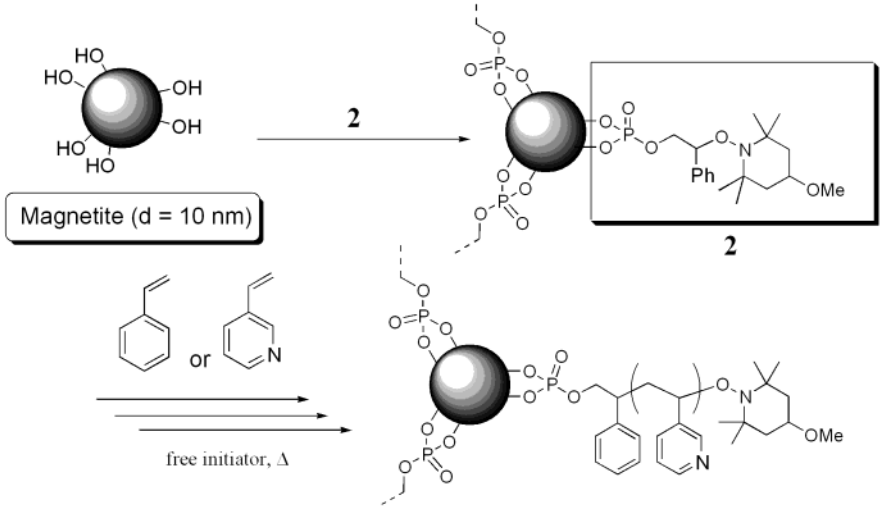

Table 1. M_n and M_w/M_n of the Grafted PS and the PS Polymerized from the Free Initiator

no.	convn, %	M_n(surface)	M_w/M_n(surface)	M_n(free)	M_w/M_n(free)
1	27.1	12 300	1.27	12 000	1.26
2	28.8	13 100	1.30	13 200	1.27
3	94.5	42 000	1.27	40 000	1.29

Table 2. M_n and M_w/M_n of the P3VP Polymerized from the Free Initiator

no.	convn, %	monomer:free initiator	M_n	M_w/M_n
1	81.2	523:1	21 400	1.60
2	87.5	523:1	21 600	1.69
3	61.2	350:1	11 200	1.53
4	75.8	350:1	16 500	1.46

surface area of magnetite was estimated assuming magnetite particles to be spheres with diameters of 10 nm and densities of 5.18 g/cm^3 for a whole particle.

The graft densities of PS or P3VP on magnetite particles were estimated to be 0.12−0.20 chains/nm^2. These graft densities were relatively high compared with the "grafted-to" method.[6] The density of surface initiator **2** was 0.73 chains/nm^2. It therefore can be concluded that 16−27% of initiator on the magnetite surface participated in the polymerization.

Characterization of Polymer-Grafted Magnetite. To examine the dispersibility and stability of the polystyrene-grafted magnetite in organic solvents, the modified magnetite nanoparticles were added to chloroform and dispersed by ultrasonic wave for 10 min. The dispersibility and stability were evaluated by ultraviolet−visible (UV−vis) spectroscopy.

In the case of unmodified magnetite particles, the absorbance decreased over time because the magnetite particles aggregated by magnetic interactions and precipitated to the bottom of the UV cell. Finally, the absorbance reached almost 0 by centrifugation over a longer period of time. In contrast, in the case of polystyrene-modified magnetite, even after centrifugation, absorbance decreased slightly over several hours. In other good solvents such as THF, toluene, and ethyl acetate, PS-grafted magnetite nanoparticles were also stably dispersed. In poor solvents such as hexane, methanol, and acetone, they were not stably dispersed. These results indicate that the dispersibility and stability are influenced by the solubility of the grafted PS. As such, steric repulsion among polystyrene chains on the magnetite surface blocks retards coagulation caused by magnetic interactions of the magnetite core, and the affinity of magnetite particles to chloroform is improved by the presence of polystyrene on the magnetite surface (Figure 1). The state of the modified particles depends on whether the solvent is a good solvent or a poor solvent for polystyrene.

Figure 2 shows the UV−vis spectra of P3VP-modified magnetite dispersion (a) in chloroform and (b) in pH 3.0 aqueous solution. P3VP-grafted magnetite nanoparticles were dispersed into chloroform and a weak acidic aqueous solution by sonication for 10 min. In chloroform, the spectrum did not change over several hours because chloroform is a good solvent for P3VP. Even after centrifugation, absorbance did not reach 0. In pH 3.0 aqueous solution prepared by HCl solution, the P3VP-grafted magnetite nanoparticle was dispersed, and the UV−vis spectrum did not change over several hours, similar to the results in chloroform. Even after centrifugation, the absorbance did not reach 0. This stable dispersion is due to the protonation of pyridine moieties in grafted P3PV chains. Therefore, the surface modification of nanoparticles allowed dispersion in weak acidic solution using reactive sites in the polymer chain.

Furthermore, the P3VP-grafted magnetite was quarternized by iodomethane. Quanternization of polymer chain can give high solubility of polymer chain in neutral water. The grafted magnetite and iodomethane were mixed and stirred for 2 h in methanol under nitrogen atmosphere. Figure 3 shows the UV−vis spectra of quarternized P3VP-modified magnetite dispersion in natural water. The quarternized P3VP-grafted magnetite was successfully dispersed in neutral water. The stability of the dispersion was similar to that of P3VP-grafted magnetite in chloroform and in acidic aqueous solution.

To investigate the magnetic response against an external magnetic field, UV−vis spectra were measured as a function of time after the neodymium magnet (3720 G_{max} evaluated by Gauss Meter model MG-601: Maguna Co., Ltd. Tokyo, Japan) was applied from the bottom of the cell. As shown in Figure 4, the absorbance gradually decreased both in chloroform and in pH 3.0 aqueous solution after applying the magnet. These phenomena indicated that the magnetite nanoparticles still maintain their ferromagnetism. PS-grafted mag-

Table 3. Graft Densities of PS or P3VP on Magnetite Particle

no.	sample	weight loss, %	graft density, chains/nm^2	participation of initiator moiety, %
1	PS (M_n = 12 000, M_w/M_n = 1.26)	35.1	0.19	26
2	PS (M_n = 13 200, M_w/M_n = 1.27)	37.6	0.20	27
3	PS (M_n = 40 000, M_w/M_n = 1.29)	50.9	0.12	16
4	P3VP(M_n = 16500, M_w/M_n = 1.46)	32.0	0.12	16

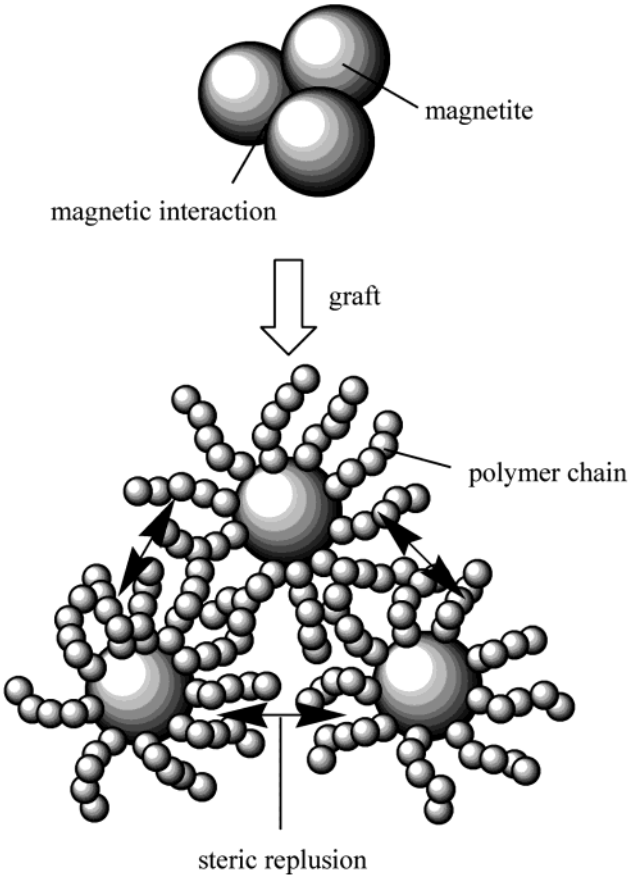

Figure 1. Illustration of polymer-grafted magnetite.

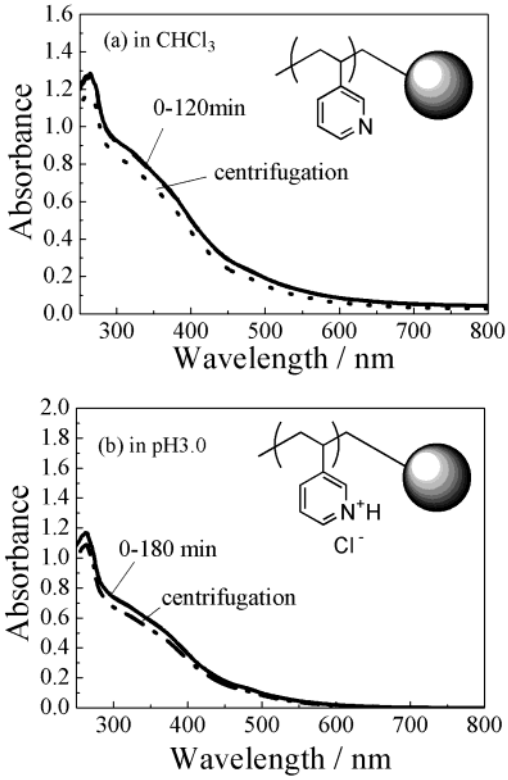

Figure 2. UV−vis spectra of poly(3-vinylpyridine)-modified magnetite (M_n = 16 500, M_w/M_n = 1.46) particles (a) in $CHCl_3$ and (b) in pH 3.0 acidic solution (0.1 mg/mL).

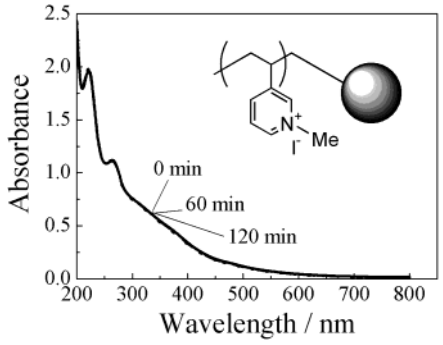

Figure 3. UV−vis spectra of quarternized poly(3-vinylpyridine)-modified magnetite (M_n = 16 500, M_w/M_n = 1.46) particles in natural water (0.1 mg/mL).

netite in chloroform showed similar results.Figure 5 shows the change in absorbance at λ = 350 nm as a function of time after the magnet was placed in chloroform dispersed PS-grafted magnetite (M_n = 12 000): d10-PS and P3VP-grafted magnetite (M_n = 16 500):d10-P3VP and pH 3.0 dispersed d10-P3VP. These absorbances were normalized as 1.0 before applying the magnet. The rates of the decrease in absorbance in pH 3.0 were faster than in chloroform. It seems that the repulsion among protonated polymer chains in pH 3.0 is most effective for stable dispersion.To obtain further insight into the aggregation state of the nanoparticles, size distributions in solution were estimated by DLS measurements. Figure 6 shows the size distributions of (a) PS-grafted magnetite in chloroform, (b) P3VP-grafted magnetite in chloroform, and (c) P3VP-grafted magnetite in pH 3.0. Table 4 shows the estimated average diameter distributions by DLS measurement and calculated diameter. The observed diameters were (a) 110 ± 16 nm in chloroform, (b) 194 ± 27 nm in chloroform, and (c) 65 ± 9 nm in pH 3.0. To estimate the dispersion state of the nanoparticles, a structure model of polymer-grafted magnetite in solution was proposed. In the case of a grafted polymer on a flat surface, the equilibrium height and morphology of the polymer were estimated by an atomic force microscope (AFM).[23] In contrast, in the case of a polymer on a nanoparticle surface, it is difficult to estimate the thickness and morphology of the grafted polymer. Because many theories[24−26] regarding grafted polymers on flat surface have been discussed, these theories were adapted for magnetite nanoparticles, as the surface is to be locally flat. Both "mushroom" and "brush" polymer grafts are known to exist on surfaces. The grafted polymer behaves as a statistical coil of typical size $R \sim aN^v$, where a is the Kuhn statistical segment length with a = 0.67 nm for a polystyrene monomer unit; N is the number of monomer units, and the scaling exponent v character-

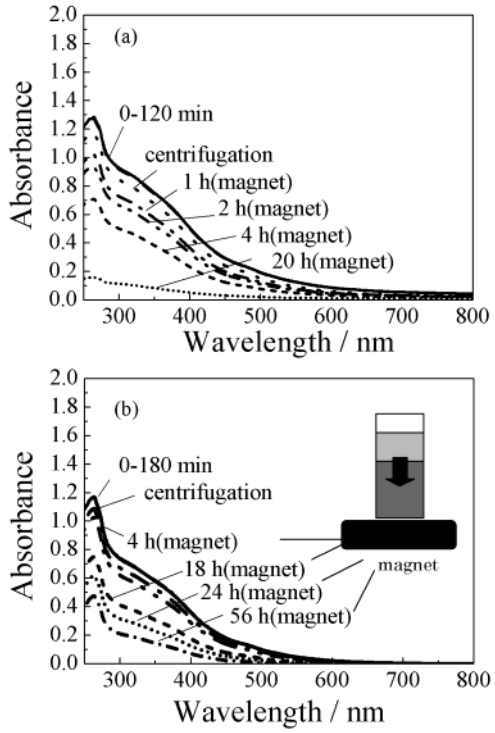

Figure 4. UV−vis spectra of P3VP-grafted magnetite (a) in chloroform and (b) in water (pH 3.0) (0.1 mg/mL). Time (magnet) shows progressed time from placing the magnet at the bottom of cell, after centrifugation.

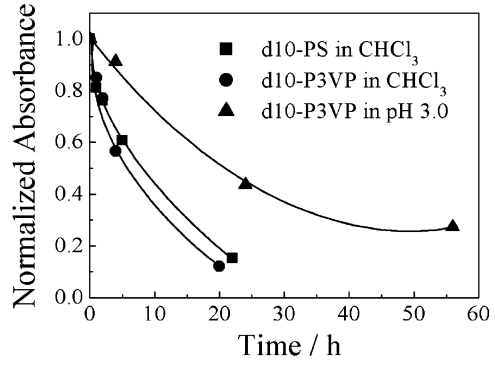

Figure 5. Decrease in normalized absorbance as a function of time after centrifugation at $\lambda = 350$ nm.

izes the solvent quality ($\nu \sim {}^3/_5$ in good solvent and ${}^1/_2$ in a Θ solvent).[27] The graft density σ and the distance between the grafting site d on the surface are related as $\sigma \sim 1/d^2$. In the "mushroom" regime, $d \gg R$ or $\sigma R^2 \ll 1$, where grafted chains do not interact, and in the "brush" regime, $d \ll R$ or $\sigma R^2 \gg 1$, where the grafted polymers are strongly overlapping and stretch away from the grafting surface to avoid unfavorable monomer−monomer contacts. To investigate the "mushroom" or "brush" types, inserting the graft density from Table 3 and R into σR^2, 25 and 23 are obtained for PS and P3VP, respectively, using the DLS measurement. Therefore, grafted polymers are assumed to be in the "brush" regime. The height h of the grafted layer is given by[28]

$$h = (12/\pi)^{1/3} N \sigma^{1/3} (\omega/\nu)^{1/3} \qquad (1)$$

where ω is the excluded volume parameter, approximately (2 Å)^3; N is the number of monomers, and $\nu = (a^3/3)^{-1}$. Inserting each value into (1), 11 and 13 nm are obtained for PS and P3VP, respectively. Therefore, the

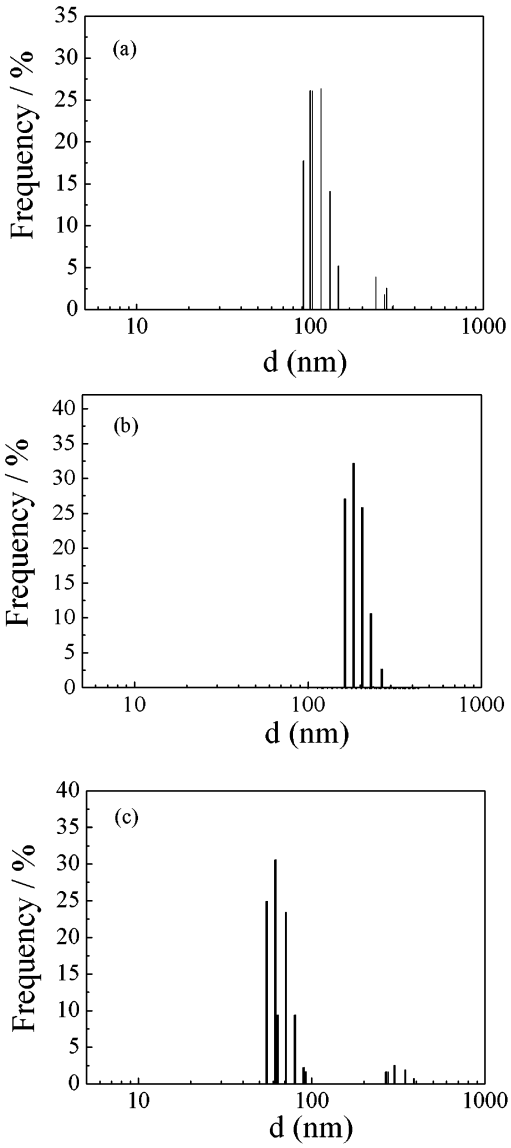

Figure 6. Size distribution of (a) PS-grafted magnetite (M_n = 12 000) in $CHCl_3$, (b) P3VP-grafted magnetite (M_n = 16 500) in $CHCl_3$, and (c) P3VP-grafted magnetite (M_n = 16 500) in pH 3.0, as estimated by DLS.

Table 4. Size Distribution Results from DLS

no.	grafted polymer	M_n	solvent	obsd diam (nm)[a]	calcd diam (nm)[b]
1	PS	12 300	chloroform	110 ± 16	32
2	P3VP	16 500	chloroform	194 ± 27	36
3	P3VP	16 500	pH 3.0 aqueous	65 ± 9	36

[a] Estimated by DLS measurement, determined by histogram fit. [b] Calculated by assuming grafted magnetite particle as a sphere 10 nm in diameter and graft polymer length obtained from eq 1.

equilibrium diameters of polymer-grafted magnetite with diameters of approximately 10 nm are 32 nm for PS and 36 nm for P3VP in good solvents. The thickness L_d in the dry state could be estimated by

$$L_d = \sigma M_n / d N_A \qquad (2)$$

where d is the bulk density of the polymer (for PS 1.04−1.065 g/cm^3)[29] and N_A is Avogadro's number.

In the dry state, the polymer thicknesses grafted on magnetite nanoparticles were found to be 3.5−3.6 and

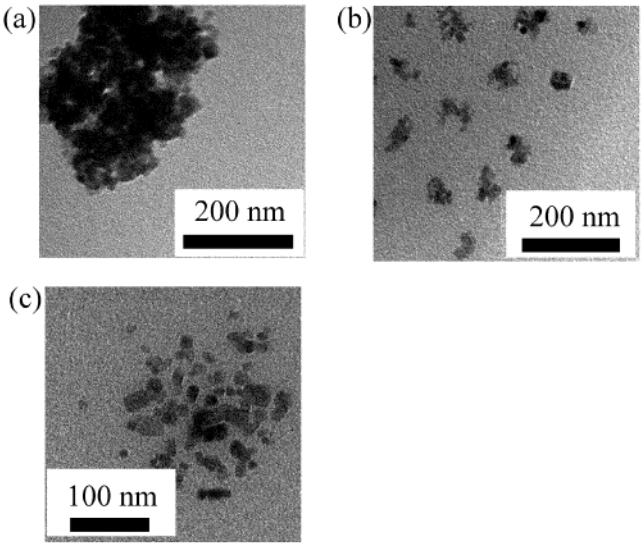

Figure 7. TEM images of (a) unmodified magnetite, (b) polystyrene-modified magnetite, dispersed at 0.01 mg/mL in $CHCl_3$, and (c) poly(3-vinylpyridine)-modified magnetite dispersed at 0.01 mg/mL in $CHCl_3$.

3.1−3.2 nm for PS and P3VP. Therefore, the heights of the grafted polymers in good solvents, as obtained by eq 1, on magnetite were approximately three to four times as large as those in the dry state, as obtained by eq 2. This elongation is in good agreement with the results of ref 23b. In that study, Fukuda et al. showed that the thickness of PMMA brushes with σ (0.14−0.42 chains/nm^2) in toluene is approximately four to seven times greater than that in the dry state. For this reason, the height h of the grafted layer obtained by eq 1 was adopted as the equilibrium diameter in good solvent. Actually, because the surface of the particles could not be considered as flat, the distance among polymer grafted on magnetite nanoparticles with diameter 10 nm could be estimated larger than that of flat surfaces and then the graft densities becomes decreasing as going outside. Therefore, it seems that the height h of the grafted layer in good solvents and the thickness L_d in the dry state on magnetite surface could be underestimated compared with flat surface.

Considering those equilibrium diameters, PS- and P3VP-grafted magnetite in chloroform were dispersed as aggregates of (a) approximately three or four particles or (b) five or six particles or, on the other hand, as aggregates of (c) approximately two particles in pH 3.0 at the magnetic response measurement condition. From the rate of decrease of normalized absorbance (Figure 5) and size distribution (Figure 6), it seems that magnetic response is influenced by the dispersion states in solutions.Figure 7 shows TEM images of (a) unmodified, (b) PS-modified, and (c) P3VP-modified magnetite particles in chloroform prepared by dropping their dispersion after sonication onto a carbon-coated copper grid. Unmodified magnetite was observed as an aggregate over several hundred nanometers by a strong magnetic interaction. In contrast, PS- and P3VP-modified magnetite particles were observed to have fine dispersion at 50 nm or less. These findings clearly reveal that the surface-initiated polymerization of styrene and 3-vinylpyridine from magnetite nanoparticles allows for dispersion and stability in appropriate solvents.

Conclusion

In summary, the authors successfully prepared PS- and P3VP-grafted magnetite particles using surface modifier **2** with both an NMRP moiety and phosphoric acid groups that can interact with Fe−OH groups on the magnetite surface. With this method, it is possible to control the length of the polymer grafted on the nanoparticle. The PS- and P3VP-grafted magnetite particles were dispersed stably in good solvents for PS or P3VP. Additionally, by protonation, P3VP-grafted magnetite nanoparticles were dispersed in acid solution, and by quarternization with iodomethane, they were dispersed in neutral aqueous solution. Finally, the polymer-grafted magnetite in the stable dispersion was applied against an external magnetic field, and the magnetic response was influenced by the dispersibility state in solution. The present method of preparation can be highly useful for other metals or metal oxides that can interact strongly with a phosphoric acid group.

Acknowledgment. The authors would like to thank Prof. K. Enpuku (Kyushu University) for providing magnetite particles. R.M. acknowledges the financial support of a Grant-in-Aid for JSPS Fellows. This work was partially supported by a Grant-in-Aid for the 21st century COE Program "Functional Innovation of Molecular Informatics" from the Ministry of Education Culture, Science, Sports, and Technology of Japan.

References and Notes

(1) (a) Usuki, A.; Kawasumi, M.; Kojima, Y.; Fukushima, Y.; Okada, A.; Kurauchi, T.; Kamigaito, O. *J. Mater. Res.* **1993**, *8*, 1172. (b) Kojima, Y.; Usuki, A.; Kawasumi, M.; Okada, A.; Fukushima, Y.; Kurauchi, T.; Kamigaito, O. *J. Mater. Res.* **1993**, *8*, 1185.
(2) (a) Gent, A. N.; Hsu, E. C. *Macromolecules* **1974**, *7*, 933. (b) Kondo, A.; Urabe, T.; Yoshinaga, K. *Colloids Surf. A: Physicochem. Eng. Aspects.* **1996**, *109*, 129.
(3) (a) Ulman, A. *Chem. Rev.* **1996**, *96*, 1533. (b) Schaaff, T. G.; Whetten, R. L. *J. Phys. Chem. B.* **2000**, *104*, 2630. (c) Yonezawa, T.; Onoue, S.; Kimizuka, N. *Langumuir* **2001**, *17*, 2291.
(4) Yamamoto, K.; Otsuka, H.; Wada, S.-I.; Takahara, A. *Chem. Lett.* **2001**, 1162.
(5) (a) Van Alsten, J. G. *Langmuir* **1999**, *15*, 7605. (b) Nakamae, K.; Tanigawa, S.; Sumiya, K.; Matsumoto, T. *Colloid Polym. Sci.* **1988**, *266*, 1015. (c) Yee, C.; Kataby, G.; Ulman, A.; Prozorov, T.; White, H.; King, A.; Rafailovich, M.; Sokolov, J.; Gedanken, A. *Langmuir* **1999**, *15*, 7111.
(6) Ben Ouada, H.; Hommel, H.; Legrand, A. P.; Balard, H.; Papirer, E. *J. Colloid Interface Sci.* **1988**, *122*, 441.
(7) Boven, G.; Oosterling, M. L. C. M.; Challa, G.; Jan, A. *Polymer* **1990**, *31*, 2377.
(8) (a) Prucker, O.; Rühe, J. *Macromolecules* **1998**, *31*, 592. (b) Prucker, O.; Rühe, J. *Macromolecules* **1998**, *31*, 602.
(9) (a) Ejaz, M.; Ohno, K.; Tsujii, Y.; Fukuda, T. *Macromolecules* **2000**, *33*, 2870. (b) Ohno, K.; Koh, K.-M.; Tsujii, Y.; Fukuda, T. *Macromolecules* **2002**, *35*, 8989.
(10) Quirk, P. P.; Mathers, R. T.; Cregger, T.; Foster. M. D. *Macromolecules* **2002**, *35*, 9964.
(11) (a) Zhou, Q.; Fan, X.; Xia, C.; Mays, J.; Advincula, R. *Chem. Mater.* **2001**, *13*, 2465. (b) Zhou, Q.; Wang, S.; Fan, X.; Advincula, R.; Mays, J. *Langmuir* **2002**, *18*, 3324.(c) Fan, X.; Zhou, Q.; Cristofoli, W.; Advincula, R. *Langmuir* **2002**, *18*, 4511. (d) Advincula, R.; Zhou, Q.; Park, M.; Wang, S.; Mays, J.; Sakellariou, G.; Pispas, S.; Hadjichristidis, N. *Langmuir* **2002**, *18*, 8672.
(12) Hawker, C. J. *J. Am. Chem. Soc.* **1994**, *116*, 11185.
(13) (a) Jung Chu, W.; Jacobs, P. *Magn. Reson. Imaging* **1995**, *13*, 661. (b) Jung Chu, W. *Magn. Reson. Imaging* **1995**, *13*, 675.
(14) Kammel, M.; Hoell, A.; Wiedenmann, A. *Scr. Mater.* **2001**, *44*, 2341.
(15) Pardoe, H.; Chua-anusorn, W.; Pierre, T. G. St.; Dobson, J. *J. Magn. Magn. Mater.* **2001**, *225*, 41.

(16) Radulescu, M. M. *J. Magn. Magn. Mater.* **1990**, *85*, 144.
(17) Kang, Y. S.; Risbud, S.; rabolt, J.; Stroeve, P. *Langmuir* **1996**, *12*, 4345.
(18) (a) Enpuku, K.; Hotta, M.; Nakahodo, A. *Physica C* **2001**, *357*−*360*, 1462. (b) Enpuku, K.; Minotani, T.; Gima, T.; Kuroki, Y.; Itoh, Y.; Yamashita, M.; Katakura, Y.; Kuhara, S. *Jpn. J. Appl. Phys.* **1999**, *38*, L1102.
(19) Ding, X. Z.; Fischer, A.; Brembilla, A.; Lochon, P. *J. Polym. Sci., A. Polym. Chem.* **2000**, *38*, 3067.
(20) Hawker, C. J. *Acc. Chem. Res.* **1997**, *30*, 373.
(21) Hawker, C. J.; Barclay, G. G.; Dao, J. *J. Am. Chem. Soc.* **1996**, *118*, 11467.
(22) Chalari, I.; Pispas, S.; Hadjichristidis, N. *J. Polym. Sci., A. Polym. Chem.* **2001**, *39*, 2889.
(23) (a) Yamamoto, S.; Ejaz, M.; Tsujii, Y.; Matsumoto, M.; Fukuda, T. *Macromolecules* **2000**, *33*, 5602. (b) Yamamoto, S.; Ejaz, M.; Tsujii, Y.; M.; Fukuda, T. *Macromolecules* **2000**, *33*, 5608. (c) Yamamoto, S.; Tsujii, Y.; Fukuda, T. *Macromolecules* **2000**, *33*, 5995.
(24) (a) de Gennes, P. G. *Macromolecules* **1980**, *13*, 1069. (b) de Gennes, P. G. *Adv. Colloid Interface Sci.* **1987**, *27*, 189.
(25) (a) Milner, S. T. *Science* **1991**, *251*, 905. (b) Milner, S. T.; Witten, T. A.; Cates, M. E. *Macromolecules* **1988**, *21*, 2610.
(26) Marques, C.; Joanny, J.-F.; Leibler, L. *Macromolecules* **1988**, *21*, 1051.
(27) Barrat, J.-L.; Joanny, J.-F. *Adv. Chem. Phys.* **1996**, *94*, 1.
(28) Eq 1 was listed in: Jordan, R.; Ulman, A.; Kang, J. F.; Rafailovich, M. H.; Sokolov, J. *J. Am. Chem. Soc.* **1999**, *121*, 1016.
(29) Brandrup, J., Immergut, E. H., Eds. *Polymer Handbook*; John Wiley & Sons: New York, 1989.

MA035523G